IB-1739



**Thomas Rohr**
**Cong Yu**
**Mark H. Davey**
**Frantisek Svec**
**Jean M. J. Fréchet**

Department of Chemistry,
University of California
and E.O. Lawrence Berkeley
National Laboratory,
Materials Sciences Division,
Berkeley, CA, USA

# Porous polymer monoliths: Simple and efficient mixers prepared by direct polymerization in the channels of microfluidic chips

Porous monolithic polymers have been prepared by photoinitiated polymerization of mixtures consisting of 2-hydroxyethyl methacrylate, ethylene dimethacrylate, UV-sensitive free radical initiator and porogenic solvent within channels of specifically designed microfluidic chips and used as micromixers. Substituting azobisisobutyronitrile with 2,2-dimethoxy-2-phenylacetophenone considerably accelerated the kinetics of the polymerization. Mixtures of cyclohexanol and 1-dodecanol and of hexane and methanol were used, respectively, to control the porous properties and therefore the mixing efficiency of the device. The performance of the monolithic mixers has been tested by pumping aqueous solutions of two fluorescent dyes at various flow rates and monitoring the point at which the boundary of both streams completely disappears. Best results were achieved with a monolithic mixer containing very large irregular pores.

**Keywords:** Microfluidics / Microchip / Porous polymer / Monolith / Mixer EL 4603

## 1 Introduction

Analytical microfluidic chip-based devices are expected to considerably facilitate analytical operations in terms of increased speed, higher throughput, and lower costs. However, these benefits can only be achieved through the integration of several devices performing a variety of analytical protocols in a single chip, thereby creating the micro total analytical system (μ-TAS) [1,2]. Microfluidic chip technologies have already been used successfully in a variety of applications. However, almost all of today's microchips include open channels architectures or channels containing features created by standard microfabrication methods [3].

One of the persisting problems of microfluidic chip technologies is the lack of efficient mixing within the channels. Such mixing is required for success in a number of operations such as sample injection, gradient elution, *in situ* derivatization, and chemical reactions. Mixing of components originally residing in separate phases is always achieved as a result of diffusion-powered trafficking between these phases. Turbulent flow generally accelerates mixing since it physically splits the streams in smaller segments thus making the diffusional path shorter. However, the very confined space within the microchannels makes it difficult to achieve the high Reynolds numbers required for turbulent flow. As a result, the flow typically observed in microchannels is laminar [4, 5]. Therefore, mixing devices must be developed and incorporated in the microfluidic devices.

The simplest solution to the mixing problem is the use of a T-piece [6, 7]. For example, Jacobson *et al.* [7] demonstrated parallel mixing at various mixing ratios using a series of T-intersections. However, this approach does not address the lack of turbulences and mixing within a reasonable channel length can only be achieved at low flow velocities. An increase in mixing efficiency has been observed after dividing both phases into a larger number of small parallel channels, mixing the streams in each of these channels, and recombining the substreams again into a single channel. In this approach, enhancement of the mixing results from the increase in contact area between the two phases [8]. A somewhat similar strategy involves splitting the streams in an array of small laminae followed by their recombination in a triangular chamber [9]. Regnier [10] recently introduced a picoliter-volume mixer with a wave-like architecture that includes multiple intersecting channels of varying lengths having a bimodal width distribution. This approach enhances both lateral and longitudinal mixing and the device is very efficient. A three-dimensional serpentine channel enables mixing at higher Reynolds numbers [11]. The manufacture of all of the micromixers discussed above involves the use of typical microfabrication techniques. Both rather complex designs and very small features can easily be fabricated

**Correspondence:** Professor Jean M. J. Fréchet, University of California, Department of Chemistry, Berkeley, CA, USA
**E-mail:** frechet@cchem.berkeley.edu
**Fax:** +510-643-3079

**Abbreviations:** **AIBN**, 2,2'-azobisisobutyronitrile; **DAP**, 2,2-dimethoxy-2-phenylacetophenone; **EDMA**, ethylene dimethacrylate; **HEMA**, 2-hydroxyethyl methacrylate; **SEM**, scanning electron microscope

≈ WILEY-VCH Verlag GmbH, 69451 Weinheim, 2001

0173-0835/01/1810–3959 $17.50+.50/0

in substrates such as glass or silicon. However, production of devices with very fine features using polymer-based substrates and the use of fabrication techniques such as hot embossing and injection molding is still lagging.

The rigid porous monoliths prepared *in situ* by thermally initiated polymerization processes we introduced in the early 1990s have already been used in a number of applications including chromatographic separations, solid-phase extraction, scavenging, polymer-supported reactions, catalysis and nonmechanic valves [11–17]. Our previous studies have also demonstrated that the porous properties of the monolithic polymers can be controlled within a broad range. However, the thermally initiated free radical polymerization used originally was not well suited for the preparation of monolithic structures within microdevices since selective heating of specific areas of the microchip to locate the monolith strictly within the assigned space is relatively difficult to achieve. This issue was subsequently addressed by the development of UV initiated polymerization processes [18–20] similar to the photolithographic patterning used in microelectronics. Photopolymerization enables the formation of monoliths only within a specified space. The polymerization reaction is strictly confined within the areas exposed through a mask, while no polymerization occurs in unexposed zones.

The internal structure of our porous polymer monoliths is bimodal and consists of an array of interconnected microglobules and pores. While the beds packed with almost uniform beads used in chromatographic columns promote longitudinal mixing, lateral mixing requires a more heterogeneous morphology of the porous body [10]. Since the process used for the preparation of monolithic materials enables a broad range of variations of their porous properties and internal morphology and is easily amenable to the microchip format, the porous monoliths appear to be well suited for the preparation of mixing microdevices. In this report, we demonstrate the suitability of our porous polymer monoliths prepared by on-chip UV initiated polymerization for the fabrication of simple and efficient micromixers.

## 2 Materials and methods

### 2.1 Materials

Ethylene dimethacrylate (98%, EDMA), 2-hydroxyethyl methacrylate (97%, HEMA), 2,2'-azobisisobutyronitrile (98%, AIBN), 2,2-dimethoxy-2-phenylacetophenone (99%, DAP), 1-dodecanol (98%), cyclohexanol (99%), 5-(6)-carboxyfluorescein (99%), rhodamine B (80%), sodium tetraborate decahydrate (99.5%) and 3-(trimethoxysilyl)propyl methacrylate (98%) were purchased from Aldrich (Milwaukee, WI, USA). Basic alumina (Brockman activity I, 60–325 mesh), sodium hydroxide (98%) and hydrochloric acid (37.5%) were obtained from Fisher Scientific (Pittsburgh, PA, USA). Methanol (99.8%) and acetone (99.5%) were purchased from EM Science (Gibbstown, NJ, USA). The monomers EDMA and HEMA were purified by passing them through a bed of basic alumina to remove inhibitors and distilled under reduced pressure. All other chemicals were used in the highest quality without further purification.

### 2.2 Preparation of monolithic mixers

The microchip used in this study is shown schematically in Fig. 1a and b. It contains one straight channel with a width of 200 μm and a depth of 50 μm that branches in two side channels. These microchips were made from Borofloat glass wafers (diameter 100 mm, thickness 1.1 mm; Precision Glass & Optics, Santa Ana, CA, USA) in the microfabrication laboratory of the University of California at Berkeley. The detailed procedure for their fabrication was reported elsewhere (Yu *et al.*, submitted).

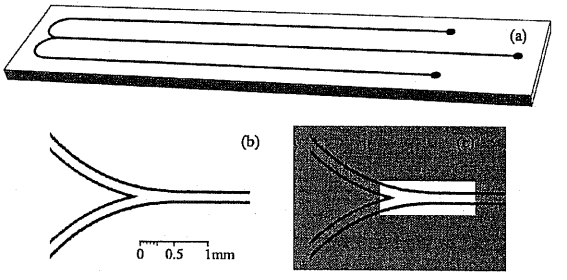


**Figure 1.** (a) Schematics of the microchip layout, (b) magnified view of channels at the mixing area, (c) position of the photo mask used for the preparation of the monolithic mixer.

#### 2.2.1 Surface modification of channels

The channels were rinsed with acetone and water using a syringe, activated with 0.2 mol/L sodium hydroxide for 30 min, washed with water followed by 0.2 mol/L HCl for 30 min, then with water again, acetone, and dried at 120°C for 1 h. The channel was filled with a 30 vol.% acetone solution of 3-(trimethoxysilyl)propyl methacrylate, sealed, and left to react for 24 h at room temperature. The modified microchips were washed with acetone and dried.

### 2.2.2 *In situ* photopolymerization

The monomer mixtures shown in Table 1 were purged with nitrogen gas for 5 min. The top of the microchip was covered with a mask as shown in Fig. 1c, the channels filled with the deaerated polymerization mixture using a syringe, and the microchip was exposed to UV-light from an Oriel deep UV illumination system series 8700 (Stratford, CT, USA) fitted with a 500 W HgXe-lamp. The radiation power was measured using an OAI Model 354 exposure monitor (Milpitas, CA, USA). Table 2 shows the radiation power of this UV lamp measured with several probe heads. After the desired polymerization time elapsed, the chip was aligned between two aluminum plates with the top one containing holes suitable for the attachment of chromatographic fittings, connected to a syringe pump (model 100 DM: ISCO, Lincoln, NE, USA), and the channels were washed with methanol for 12 h at a flow rate of 1 μL/min. The flow resistance (back pressure) was then measured for flow rates in the range of 0.1–3 μL/min. Finally, the chip was removed from the holder and fused-silica capillaries (Polymicro Technologies, Phoenix, AZ, USA) were affixed to its holes using a two-component epoxy glue.

**Table 1.** Composition of polymerization mixtures in weight percents and reaction times used for the *in situ* preparation of monolithic mixers

| Polymer | 1 | 2 | 3 | 4 | 5 | 6 |
|---|---|---|---|---|---|---|
| 2-Hydroxyethyl methacrylate | 24 | 24 | 24 | 9 | 6 | 3 |
| Ethylene dimethacrylate | 16 | 16 | 16 | 6 | 4 | 2 |
| 1-Dodecanol | 42 | – | – | 41.1 | 43.5 | 45.9 |
| Cylohexanol | 18 | – | – | 43.9 | 46.5 | 49.1 |
| Methanol | – | 30 | 30 | – | – | – |
| Hexane | – | 30 | 30 | – | – | – |
| DAP [a] | 1 | – | 1 | 1 | 1 | 1 |
| AIBN [a] | – | 1 | – | – | – | – |
| Reaction time (min) | 6 | 60 | 60 | 20 | 30 | 40 |

a) Percentage of initiator with respect to the monomers

**Table 2.** Radiation power of the UV–lamp as measured with different probe heads used for the *in situ* preparation of monolithic mixers

| Wavelength (nm) | Radiation power (mW/cm$^2$) |
|---|---|
| 254 | 8.16 |
| 260 | 11.15 |
| 280 | 2.31 |
| 310 | 6.32 |
| 365 | 2.83 |
| 400 | 3.92 |
| 436 | 2.25 |

## 2.3 Porosity measurements

Since the amount of porous polymer prepared in the microchannels is not sufficient for porosimetry measurement, a mold with a larger volume, yet with properties similar to those of the actual microchip was used for bulk polymerization. This mold consisted of a circular Teflon base plate and a 4" Borofloat glass wafer (the same as that used for the fabrication of microchips) separated by a 700 μm thick polysiloxane gasket and held together using C-clamps. The mold was filled with the remainder of the polymerization mixtures shown in Table 1 and polymerized under the same conditions used for the preparation of monolithic mixers. After the polymerization has been completed, the mold was opened, the solid polymer recovered, broken into somehow smaller pieces, extracted in a Soxhlet apparatus for 12 h, and dried in a vacuum oven at 60°C for 12 h. The pore size distributions of the porous monolithic materials were determined using an Autopore III 9400 mercury intrusion porosimeter (Micromeritics, Norcross, GA, USA). Scanning electron microscope (SEM) images were obtained using an ISI high resolution analytical scanning electron microscope DS130C (Topcon, Japan).

**Table 3.** Porous properties obtained from mercury intrusion porosimetry for monoliths prepared from the polymerization mixtures shown in Table 1

| Polymer | 1 | 2 | 3 | 4 | 5 | 6 |
|---|---|---|---|---|---|---|
| Total intrusion volume (mL/g) | 1.28 | 1.30 | –[a] | –[a] | –[a] | –[a] |
| Median pore diameter (μm) | 1.0 | 10.7 | –[a] | –[a] | –[a] | –[a] |
| Porosity (%) | 50 | 50 | 50[b] | 79[b] | 86[b] | 93[b] |
| Back pressure[c] (MPa) | 0.9 | 0.01 | 0.06 | 0.09 | 0.03 | 0.005 |

a) The monolith prepared in bulk collapsed and could not be used for mercury porosimetry.
b) Value estimated from the percentage of porogenic solvent in the polymerization mixture.
c) Back pressure at a flow rate of 1 μL/min recalculated to a monolith length of 1 cm.

## 2.4 Mixing

Mixing of the two phases in the microchip was observed in an inverted microscope (Nikon Eclipse TE200) equipped with a multiband dual FITC-Texas Red epi-fluorescence filter block and a 4× objective. Solutions of two fluorescence dyes, 5(6)-carboxyfluorescein (0.05 mmol/L) and Rhodamine B (0.125 mmol/L), both in 10 mmol/L borate buffer in 3:1 methanol-water, pH 9.2, were pumped simul-

taneously through each of the channels at equal flow rates using a double syringe pump (Model 101; kd Scientific, New Hope, PA, USA). The mixing length was determined visually. Using the stage, the field observed through the microscope was moved down the channel to the point at which complete mixing characterized by a homogeneous orange-brown color all across the channel was observed. This procedure was repeated at least two times and the average value used as the mixing length. Although not exact, this method is reproducible with an error of less than $\pm$ 0.5 mm.

## 3 Results and discussion

### 3.1 Preparation of monolithic mixers

A main objective of our initial study of monolithic mixers was the mixing of aqueous solutions. Therefore, the major component of all polymerization mixtures used for the preparation of monoliths was a hydrophilic monomer, 2-hydroxyethyl methacrylate. Theoretical considerations [8–10] suggest that pore size and distribution may have a considerable effect on the mixing ability of the monoliths. In order to segregate the effects of pore size, pore volume, and morphology of the monolithic mixer, two series of monolithic materials were prepared using polymerization mixtures and conditions summarized in Table 1. A monomer:cross-linker ratio of 6:4 was used in all of these polymerizations that only differed in the composition of the porogenic solvent, type of initiator, and polymerization time.

#### 3.1.1 Kinetics of UV-initiated polymerization

Figure 2a shows the effect of reaction time on conversion of monomers using AIBN as the initiator and a radiation power of 2.6 – 19.7 mW/cm$^2$ at 260 nm. The polymerization is relatively slow and complete conversion is only achieved after more than 90 min. In contrast, the use of dimethoxyacetophenone as the UV initiator affords a much faster polymerization with complete conversion achieved within 10 min, even at the lowest radiation power (Fig. 2b). This acceleration is important for the future manufacture of microfluidic devices since it is desirable to fabricate large numbers of microchips in a shortest possible period of time.

#### 3.1.2 Control of porous properties

Obviously, the permeability of a porous polymer monolith – an important feature of the material intended for the flow-through applications – depends on its porous properties. We have demonstrated several times in the past that both the flow resistance of monoliths in HPLC mode [21] and the flow velocity in monolithic CEC columns [18, 22] is inversely proportional to the pore size. Therefore, it is extremely important to control the porous properties in order to obtain monolithic devices with the desired flow properties. In our previous studies [18, 21], we have also demonstrated that the porosity of the monolith could be controlled by adjusting the composition and percentage of porogenic solvents in the polymerization mixture. Although a similar tool can be used in the UV-initiated polymerization, the effect is not identical. The porous properties are affected by the changes in solvency of the porogenic solvents that, in turn, depends on the temperature [23]. Since the UV-initiated polymerization proceeds at room temperature, the pore size distributions are quite different from those obtained for thermally polymerized monoliths.

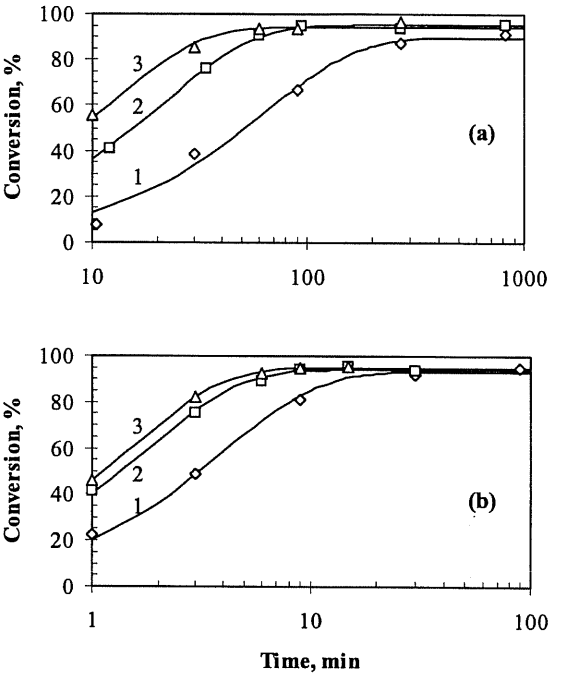


**Figure 2.** Conversion of free radical polymerization of HEMA and EDMA mixture using (a) azobisisobutyronitrile and (b) dimethoxyacetophenone initiated by UV light at a 260 nm radiation power of 2.6 (curve 1), 11.2 (curve 2) and 19.7 mW/cm$^2$ (curve 3).

First, we used mixtures of cyclohexanol and 1-dodecanol as a porogenic solvent since they proved to be very efficient in our previous research [21]. Figure 3 shows the effect of 1-dodecanol on the porous properties of UV polymerized monoliths. Clearly, an increase in percentage

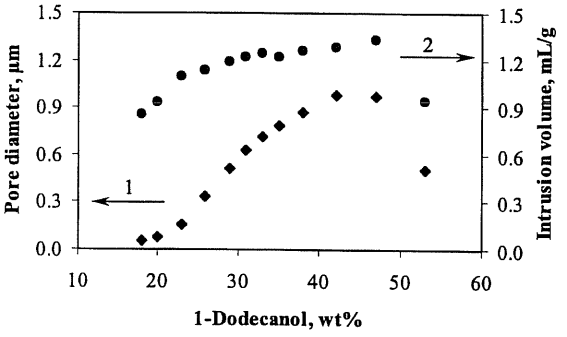


**Figure 3.** Effect of 1-dodecanol on modal pore diameter (1) and pore volume (2) of monoliths prepared from mixtures of 24% HEMA, 16% EDMA, *x*% 1-dodecanol, and (60-*x*)% cyclohexanol using UV polymerization initiated by dimethoxyacetophenone at a 260 nm radiation power of 11.2 mW/cm$^2$.

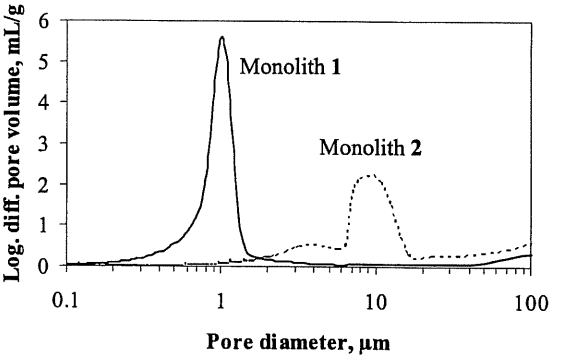


**Figure 4.** Pore size distribution profiles for monoliths **1** and **2**.

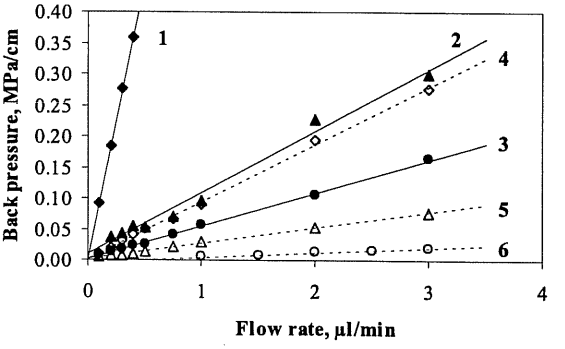


**Figure 5.** Back pressures normalized to a length of 1 cm induced by monoliths **1**, **2**, **3**, **4**, **5**, and **6** at different flow rates.

of the aliphatic alcohol in the mixture from 20 to 45% leads to an increase in pore size from less than 50 nm to over 1.1 µm. As expected, the composition of the porogenic mixture has a much smaller effect on the overall pore volume. However, these experiments also suggest that the cyclohexanol/dodecanol mixture is not suitable for the preparation of monoliths with pores larger than about 1 µm from HEMA and EDMA.

In an unrelated study (Yu *et al.*, in preparation) we developed a new porogenic mixtures that enable the preparation of monoliths with pore sizes in the range of several micrometers using UV-initiated polymerization. One of these mixtures consisting of methanol and hexane was also used for the preparation of monolithic mixers with large pores. Figure 4 illustrates the effect of this porogenic solvent on the pore size distribution profiles for monoliths **1** and **2**. Our new porogen easily affords monoliths with a modal pore size of up to 10 µm.

### 3.2 Flow resistance

The monolithic materials are typically used in the flow-through mode. Therefore, a flow resistance as low as possible is an important objective. According to the Hagen-Poiseuille law, the average laminar flow velocity $v$ through a tube of radius $r$ and length $L$ is [24]:

$$v = \frac{\Delta P r^2}{8\eta L} \quad (1)$$

where $\Delta P$ is the pressure drop along the liquid path and $\eta$ is the viscosity of the liquid. After rearranging to

$$\frac{\Delta P}{L} = \frac{8v\eta}{r^2} \quad (2)$$

this equation confirms that the pressure drop per unit length is directly proportional to the flow velocity. Indeed, Fig. 5 shows that the plots of back pressure (normalized to a length of 1 cm) *vs.* flow rate in the range of 0.1–3 µL/min are straight lines. In contrast, a simple relation between the pore size of the monoliths and back pressure, as would be predicted by Eq. (2) for a channel of radius $r$, cannot be determined. This results from the specific morphology of the monoliths used in this study (*vide infra*). However, Fig. 5 also demonstrates that the general concept of low back pressure in monoliths featuring larger pores also applies to our micromixers.

Although the lower mechanical integrity of some free standing monoliths (Table 1) prepared in the mold from polymerization mixtures containing high percentages of porogen does not enable direct determination of the pore size distribution using the extreme conditions of mercury porosimetry, these monolithic materials are mechanically stable when located in the microchannel as a result of their covalent attachment to the walls. This is

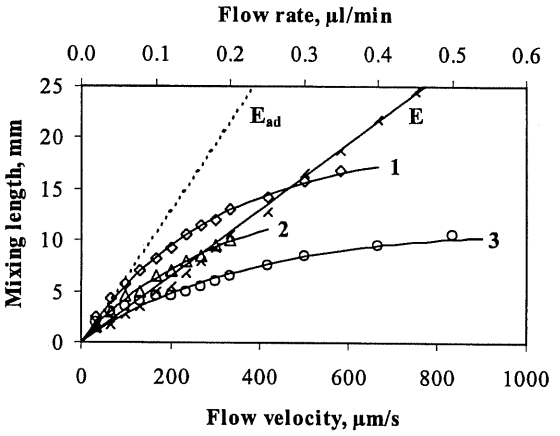


**Figure 6.** Length of the flow path required to achieve complete mixing in an empty channel (E), and channel containing porous polymer monoliths **1**, **2,** and **3.** The dashed line ($E_{ad}$) represents the length calculated for an empty channel with a cross section adjusted to 50%.

confirmed by experiments at varying and repeated cyclic changes in flow rates through the monolithic device, which do not lead to changes in the back pressure that would indicate damage of the monolithic structure.

### 3.3 Open channel

Mixing experiments in the open channel revealed a linear relationship between the flow velocity and the mixing length for the open channel. Figure 6 confirms that the experimental points fit a straight line ($r^2$ = 0.996). This is expected since mixing in the open channel occurs almost exclusively as a result of diffusion. While the time required for both compounds to diffuse and reach equal concentrations across the channel remains constant, the path length the liquid travels through the channel increases linearly with the flow velocity. As a result, longer mixing length is required at higher flow rates.

The monolith placed inside the channel occupies a specific fraction of its space. Therefore, the overall cross section through which the liquids can flow is lower than that of the open channel. This affects the flow velocity defined as flow rate divided by cross section. In order to achieve equal flow velocities in both open and monolithic mixers, the flow rate in the open channel has to be adjusted appropriately. Since all of our porous materials have a porosity of 50% or more, the actual flow velocities always lie between those for an open channel and those for a channel with a cross section half the size. Figure 6 also shows the path length required for diffusional mixing calculated for a channel that would have 50% of the actual cross section of the open channel. The path length is larger as a result of the higher flow velocity.

### 3.4 Effect of pore size

Although the median pore sizes determined by mercury intrusion porosimetry for monolithic materials **1** and **2** shown in Table 3 differ dramatically, both monoliths have very similar pore volume of 1.3 mL/g with a porosity of 50%. SEM micrographs of Fig. 7 unveil that monolith **1**

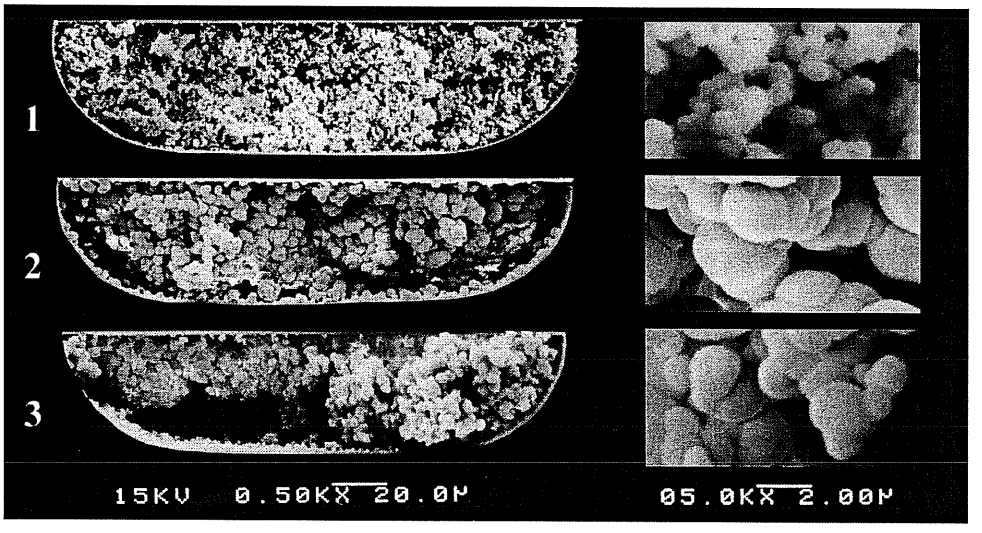


**Figure 7.** SEM images of monolithic mixers prepared from polymerization mixtures **1, 2,** and **3.**

has a larger number of smaller pores while the pores in monolith **2** are larger and less numerous. Therefore, these monoliths enable the assessment of the effect of pore size on mixing. In contrast to the mixing in the open channel, the mixing length for monolithic mixers illustrated in Fig. 6 is no longer a linear function of flow velocity but rapidly deviates from linearity. The effect of the monolithic mixers is only marginal at velocities below 50 μm/s for which diffusion prevails. However, mixing is considerably accelerated at increased flow velocities. The mixing lengths determined for the monolithic mixer **1** are about 30% longer than those found for monolith **2**. It is worth noting that the mixing length is always shorter for the channel containing a monolith than that calculated for the open channel assuming that only 50% of the cross section is available for the flow. This demonstrates that the porous monolith indeed contributes to mixing. For example, at a flow velocity of 250 μm/s, mixing lengths of 11 mm and 8 mm are characteristic of monolithic polymers **1** and **2**, respectively, while this length would be 17 mm to achieve mixing in the open channel.

The mixer prepared from polymer **3** exhibited the best performance in this series of monoliths. A mixing length of 5.5 mm at a flow velocity of 250 μm/s and less than 10 mm at flow velocities up to 850 μm/s was sufficient for complete mixing. The overall porosity of this monolith is assumed to be similar to that of monoliths **1** and **2** since monolith **3** was prepared from a polymerization mixture containing the same percentage of porogenic solvent. Compared to monolith **2** it differs only in the initiator used for polymerization. However, its morphology is rather different from those of polymers **1** and **2**. SEM micrograph of Fig. 7 shows that the monolithic structure of **3** is characterized by the presence of hollow areas as large as 30 μm in addition to the typical macroporous regions.

### 3.5 Effect of pore volume

The results achieved with monolithic mixer **3** indicate that structures containing large pores have a positive effect. Since it is difficult to increase the pore size while keeping the percentage of monomers at 40%, we achieved the desired effect by increasing the pore volume using a higher percentage of the porogenic solvent in the polymerization mixture. Although the resulting monoliths are more fragile when removed from their mold, their attachment to the walls of the channel warrants their reliable function.

Figure 8 shows the mixing performance of more porous monoliths prepared from polymerization mixtures that include 60–95% of porogen. While the mixing length of monolith **4** prepared from a mixture containing 15% monomers is similar to that of monolith **2**, monolith **5** and **6** afford much better mixing. The plots clearly demonstrate the increased efficiency over that of all other monoliths. A mixing length of only 5 mm is sufficient even at the very high flow velocity of 850 μm/s. This mixer has an internal volume of 45 nL.

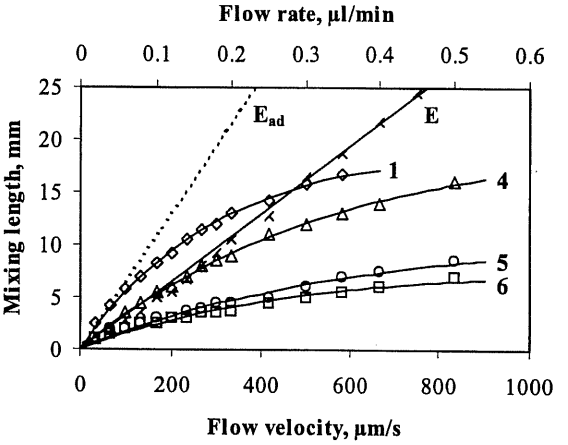


**Figure 8.** Length of the flow path required to achieve complete mixing in an empty channel (E), and channel containing porous polymer monoliths **1**, **4, 5**, and **6**. The dashed line ($E_{ad}$) represents the length calculated for an empty channel with a cross section adjusted to 50%.

The SEM images of Fig. 9 show again very large holes within the monolith. In fact, the porous polymer forms a curtain-like structure that appear to function as baffles that provide for efficient mixing even at very low flow velocities. The alternating domains of polymer and large holes force both liquid phases to flow in a meander-like path that improves the mixing. Figure 10 shows the optical micrograph of polymer **5** inside the microchannel and the erratic flow of two streams containing the fluorescent dyes. A further increase in porosity to 93% (monolith **6**) leads only to a small improvement in performance. However, the properties of this polymer were different since the polymer was prepared from a polymerization mixture in which the monomers were very diluted. These results suggest that monolith **5** has the optimal properties for the desired application.

## 4 Concluding remarks

The monolithic mixers reported in this study represent an important building block for the development of complex microanalytical systems. UV-initiated polymerization within the channels of a microfluidic device has proven

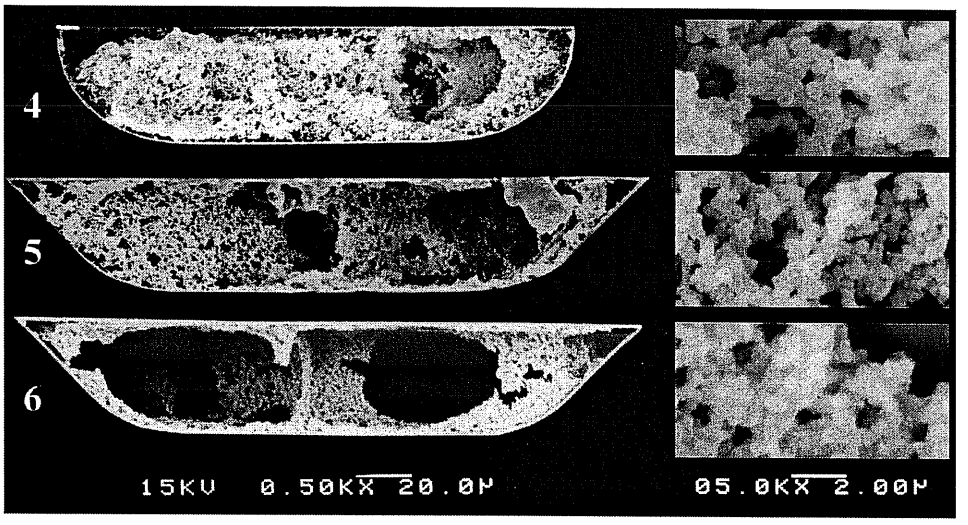


**Figure 9.** SEM images of monolithic mixers prepared from polymerization mixtures **4, 5,** and **6.**

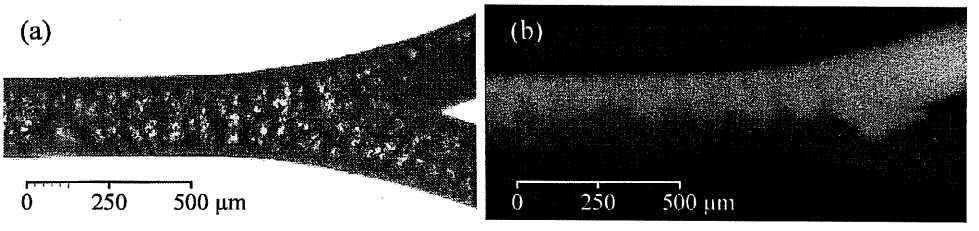


**Figure 10.** Optical micrograph of (a) polymer **5** inside the microchannel and (b) the erratic flow of two streams containing the fluorescent dyes within this monolithic mixer.

to be a simple and versatile approach that enables the single step preparation of monolithic mixers with a wide variety of porous properties at any desired location within the microchip. The monolithic devices are covalently attached to walls of the microchannel and their adequate mechanical strength and low flow resistance allow their use even in systems requiring very high flow rates. We have demonstrated in our previous research that this monolithic material is very stable and does not change its properties even after several months of continuous operation [25]. Although monolithic mixers consisting of only one monomer-cross-linker (HEMA-EDMA) combination have been demonstrated, the chemistry of the monolithic device can easily be changed by choosing different monomers. This ability to simply prepare micromixers with surface properties tuned for mixing in specific environments is an important asset in building dedicated microfluidic systems.

*This work was supported by the Office of Nonproliferation Research and Engineering of the U.S. Department of Energy under Contract No. DE-AC03-76SF00098. The authors also wish to thank Professor Juan Santiago, Stanford University, for his valuable comments and suggestions.*

Received June 25, 2001

## 5 References

[1] Manz, A., Becker, H. (Eds.), *Topics in Current Chemistry*, Vol. 194, Springer Verlag, Berlin 1998.

[2] Bruin, G. J. M., *Electrophoresis* 2000, *21*, 3931–3951.

[3] Chen, Y., Pépin, A., *Electrophoresis* 2001, *22*, 197–207.

[4] Bönkenkamp, D., Desai, A., Yang, X., Tai, Y.-C., Marzluff, E. M., Mayo, S. L., *Anal. Chem.* 1998, *70*, 232–236.

[5] Erbacher, C., Bessoth, F. G., Busch, M., Verpoorte, E., Manz, A., *Mikrochim. Acta* 1999, *131*, 19–24.

[6] Kutter, J. P., Jacobson, S. C., Ramsey, J. M., *Anal. Chem.* 1997, *69*, 5165–5171.

[7] Jacobson, S. C., McKnight, T. E., Ramsey, J. M., *Anal. Chem.* 1999, *71*, 4455–4459.

[8] Bessoth, F. G., DeMello, A. J., Manz, A., *Anal. Commun.* 1999, *36*, 213–215.

[9] Guenat, O. T., Ghiglione, D., Morf, W. E., DeRooij, N. F., *Sens. Actuat. B-Chem.* 2001, *72*, 273–282.

[10] He, B., Burke, B. J., Zhang, X., Zhang, R., Regnier, F. E., *Anal. Chem.* 2001, *73*, 1942–1947.

[11] Liu, R. H., Stremler, M. A., Sharp, K. V., Olsen, M. G., Santiago, J. G., Adrian, R. J., Aref, H., Beebe, D. J., *J. MEMS* 2000, *9*, 190–197.

[12] Svec, F., Fréchet, J. M. J., *Ind. Eng. Chem. Res.* 1999, *36*, 34–48.

[13] Peters, E. C., Svec, F., Fréchet, J. M. J., *Adv. Mat.*1997, *9*, 630–632.

[14] Peters, E. C., Petro, M., Svec, F., Fréchet, J. M. J., *Anal. Chem.*, 1997, *69*, 3646–3649.

[15] Svec, F., Fréchet, J. M. J., *Science* 1996, *273*, 205–211.

[16] Tripp, J. A., Stein, J. A., Svec, F., Fréchet, J. M. J., *Org. Lett.* 2000, *2*, 195–198.

[17] Xie, S., Svec, F., Fréchet, J. M. J., *Chem. Mat.* 1998, *10*, 4072–4078.

[18] Lämmerhofer, M., Peters, E. C., Yu, C., Svec, F., Fréchet, J. M. J., Lindner, W., *Anal. Chem.* 2000, *72*, 4614–4622.

[19] Yu, C., Svec, F., Fréchet, J. M. J., *Electrophoresis* 2000, *21*, 120–127.

[20] Viklund, C., Ponten, E., Glad, B., Irgum, K., Horsted, P., Svec, F., *Chem. Mat.* 1997, *9*, 463–471.

[21] Viklund, C., Svec, F., Fréchet, J. M. J., Irgum, K., *Chem. Mat.* 1996, *8*, 744–750.

[22] Peters, E. C., Petro, M., Svec, F., Fréchet, J. M. J., *Anal. Chem.* 1998, *70*, 2288–2295.

[23] Svec, F., Fréchet, J. M. J., *Macromolecules* 1995, *28*, 7580–7582.

[24] Bird, R. B.; Steward, W. E.; Lightfoot, E. N., *Transport Phenomena*, J. Wiley, New York 1960.

[25] Janco, M., Sykora, D., Svec, F., Fréchet, J. M. J., Schweer, J., Holm, R., *J. Polym. Sci. A, Polym. Chem.* 2000, *38*, 2767–2778.